Purification and Biochemical Characterization of Tubulin from the Budding Yeast *Saccharomyces cerevisiae*†

Ashley Davis,* Carleton R. Sage, Leslie Wilson, and Kevin W. Farrell

Department of Biological Sciences, University of California, Santa Barbara, California 93106

Received April 1, 1993; Revised Manuscript Received June 7, 1993

ABSTRACT: We describe a method for isolating milligram quantities of assembly-competent tubulin from the budding yeast *Saccharomyces cerevisiae.* The tubulin is >95% purified and free of contaminating enzyme activities. As a result, it has been possible to determine the yeast tubulin equilibrium-binding constant for Mg–GTP and the tubulin GTPase activity under nonassembling and assembling conditions. We also determined the critical concentration for yeast tubulin polymerization and found it to be significantly lower than that for bovine brain tubulin under identical conditions. Similarly, the dynamic properties both of individual yeast microtubules and of bulk microtubule suspensions were significantly different from those of bovine brain microtubules free of microtubule-associated proteins. The data suggest that the properties of the yeast tubulin may reflect the particular functional requirements of the yeast cell. With this method, it is now possible to introduce any desired tubulin gene mutation into the budding yeast and correlate the phenotypic effects of the mutation in cells with the effects of the mutation on the biochemical and polymerization properties of the tubulin.

Since cytoplasmic tubulin was first isolated (Weisenberg et al., 1968) and conditions were discovered which allowed its reassembly *in vitro* (Weisenberg, 1972), a considerable body of work from many laboratories has contributed to a detailed understanding of its biochemical properties. For example, it is now known that tubulin is a heterodimer composed of two similar but nonidentical subunits, α and β (Bryan & Wilson, 1971). The heterodimer has multiple ligand-binding sites: there are several for a wide range of antimitotic drugs such as colchicine, podophyllotoxin, taxol, and vinblastine, some of which may overlap [see Dustin (1984) and Correia (1991) for reviews]; additional sites for posttranslational modifications also exist, as tubulin can be acetylated (L'Hernault & Rosenbaum, 1985), tyrosinylated (Raybin & Flavin, 1977; Chang & Flavin, 1988), and ADP-ribosylated (Kaslow et al., 1981; Lim et al., 1985; Scaife et al., 1992).

The heterodimer also possesses two guanine nucleotide-binding sites, one per subunit. The binding site on β-tubulin, called the E-site because the bound GTP is freely exchangeable, is of particular interest, since GTP hydrolysis at this site is thought to play a central role in generating microtubule dynamic properties. Microtubules continuously exchange tubulin subunits with those in the unassembled tubulin pool by at least two behaviors, termed treadmilling (Margolis & Wilson, 1978) and dynamic instability (Mitchison & Kirschner, 1984). Both of these dynamic behaviors are thought to result from the random loss and regain of "caps" of tubulin–GTP subunits at the ends of microtubules (Carlier & Pantaloni, 1981; Mitchison & Kirschner, 1984; Farrell et al., 1987), and the energy driving both dynamic behaviors appears to come from the hydrolysis of GTP (Wegner, 1976; Mejillano et al., 1990), catalyzed by the tubulin GTPase, which is stimulated when a tubulin–GTP dimer adds to the microtubule end (Weisenberg et al., 1976; Andreu & Timasheff, 1981). Both treadmilling and dynamic instability have been observed in cells (Mitchison et al., 1986; Mitchison, 1989; Hayden et al., 1990; Rieder & Alexander, 1990) and at the very least seem to be important for mitotic spindle morphogenesis, chromosome separation, and cell shape changes [e.g., see Kirschner and Mitchison (1986) and Mitchison (1988)].

Despite this body of biochemical information, the functional importance of the ligand-binding and posttranslational modification sites on tubulin, and even the amino acid residues which define these sites, is still largely a matter of conjecture [e.g., see Sternlicht et al. (1987), Burns (1992), and Burns et al. (1993)]. To a large extent, this situation exists because of the lack of an experimental system in which tubulin biochemistry and genetics can both be studied. Biochemical studies have primarily utilized tubulin from vertebrate brain, which is a rich source of tubulin, but which is inappropriate for genetic studies. Conversely, in those systems possessing facile genetics, such as the yeasts and fungi, convenient methods for isolating biochemical quantities of tubulin have not been available. Attempts to improve the biochemical utility of *Saccharomyces cerevisiae* by overexpression of tubulin genes proved unsuccessful because the excess tubulin was lethal to the cells (Burke et al., 1989; Katz et al., 1990). Consequently, it has not been possible to exploit fully the potential of the genetic approach.

The power of the genetic approach can be readily appreciated from the body of genetic work which has identified some of the key functions of microtubules in the cell. In the yeasts and fungi, for example, the isolation of conditional-lethal tubulin gene mutants contributed to an appreciation that microtubules are essential for nuclear migration and separation [reviewed in Huffaker et al. (1987)]. Tubulin mutants with altered sensitivities to antimitotic drugs have also shown that mitosis cannot occur if the stability of spindle microtubules is altered (Oakley & Morris, 1980; Cabral, 1983), and recently, genetic suppressor analysis has led to the discovery of a third member of the tubulin gene family, γ-tubulin, which appears to function only in microtubule nucleation (Oakley & Oakley, 1989; Oakley et al., 1990).

The study of tubulin function is simplified in yeast because it possesses only two α-tubulin genes, *TUB1* and *TUB3*

† This work was supported by NIH Grants GM41751 (K.W.F.) and NS13560 (L.W.).

* To whom correspondence should be addressed. Telephone: (805) 893-3683. Fax: (805) 893-4724.

0006-2960/93/0432-8823$04.00/0

Table I: Genotypes of Relevant Yeast Strains

strain	genotype	comments	reference
FSY127	*Mat α, leu2, lys4, tub2-590, ura3*	carries truncated β-tubulin gene	Katz et al. (1989)
FY41	*Mat a, ade1, his4, leu2, trp1, TUB2, ura3*	carries stable *trp1* deletion marker	F. Winston, personal communication
FFSYY5207	*FSY127 × FY41*	source of haploids for ADY series	this report
ADY101	*HIS4/his4, leu2/leu2, LYS4/lys4, trp1/trp1, tub2-590/tub2-590, ura3/ura3*	homozygous for truncated β-tubulin genes	this report
ADY103	*HIS4/his4, leu2/leu2, LYS4/lys4, trp1/trp1, TUB2/TUB2, ura3/ura3*	wild-type for *TUB2*	this report
ADY101-pADWT	*HIS4/his4, leu2/leu2, LYS4/lys4, trp1/trp1, tub2-590/TUB2-URA3, ura3/ura3*	transformed with *TUB2* at one *tub2-590* locus	this report
CSY3-pCS3WT	*HIS4/his4, leu2/leu2, LYS4/lys4, trp1/trp1, tub2-590/tub2-590::LEU2, pCS3-TUB2, ura3/ura3*	*TUB2* carried epigenetically on pCS3 CENIII plasmid	this report

(Schatz et al., 1986), and a single β-tubulin gene, *TUB2* (Neff et al., 1983); in contrast, the multiple tubulin genes present in higher organisms, which result in multiple tubulin isoforms, would complicate interpretation of the biochemical effects of tubulin gene mutations.

Recently, Barnes et al. (1992) described a method for isolating milligram quantities of substantially enriched assembly-competent tubulin from the budding yeast *S. cerevisiae*. Although the tubulin was 50–70% purified, we found that the preparation contained both nucleic acid, which interfered with microtubule polymerization, and enzyme activities, which precluded using the tubulin for biochemical analyses of GTP binding and hydrolysis.

In the present paper, we describe an improved method for isolating tubulin from *S. cerevisiae*. The tubulin is >95% purified and is free of contaminating nucleic acids and enzyme activities. As a result, it has been possible to measure the yeast tubulin equilibrium binding constant for Mg–GTP, as well as the tubulin GTPase activity under nonassembling and assembling conditions. We also describe the *in vitro* reassembly properties of bulk microtubule suspensions and the dynamic characteristics of individual yeast microtubules. The data demonstrate that the assembly properties of yeast tubulin differ significantly from those of bovine brain tubulin and suggest that some yeast tubulin properties may be tailored to suit the specific needs of the cell.

MATERIALS AND METHODS

Yeast Strains and Cell Growth. The yeast strains used in this study are described in Table I. Strains ADY101 and ADY103 were the primary experimental strains. ADY103 is a homozygous wild-type diploid at the β-tubulin locus (*TUB2/TUB2*). ADY101 is also homozygous at the β-tubulin locus, but carries 2 copies of a gene which codes for a form of β-tubulin in which the last 12 C-terminal amino acids have been truncated (*tub2-590/tub2-590*). This strain was derived from stock FSY127, kindly supplied by Dr. Frank Solomon at MIT (Katz & Solomon, 1988).

A stable *trp1* deletion marker was introduced into strains ADY101 and ADY103 by crossing FSY127 with FY41 (Dr. Fred Winston, personal communication) to obtain the diploid FFSYY5207. This diploid was sporulated, and the tryptophan-requiring haploid progeny were further screened by the polymerase chain reaction to determine whether they carried a full-length wild-type copy of *TUB2* or the truncated version, *tub2-590*. ADY101 (*tub2-590/tub2-590*) and ADY103 (*TUB2/TUB2*), carrying the stable *trp1* deletion, were finally obtained by recrossing the tryptophan-requiring haploid progeny carrying the appropriate *TUB2* alleles.

ADY101-pADWT is a heterozygous *TUB2/tub2-590* diploid obtained from ADY101 by transplacement transformation with a *TUB2-URA3* fragment. CSY3-pCS3WT is a *tub2-590/tub2-590*::LEU2 hemizygote transformed with a *CENIII* plasmid carrying a copy of *TUB2* and a *URA3* selectable marker. Quantitative Northern and Western blot analyses showed this to reconstitute a near-diploid heterozygous state at the β-tubulin locus, similar to strain ADY101-pADWT (C. R. Sage and K. W. Farrell, unpublished data).

Strains were routinely maintained on simple dextrose (SD) medium supplemented with the appropriate metabolites (Sherman et al., 1986). Large-scale cultures were obtained by inoculating 7.5 L of late-log phase cultures (grown in SD) into 80 L of YPD medium (Sherman et al., 1986) and culturing at 30 °C in a F140 Fermicell fermenter to late-log phase (A_{600} = 10). Cells were harvested with a precooled continuous-flow rotor (Sharples) to yield 1.5–2.2 kg of cells wet weight per 88 L of culture. The cell pellets were stored at 4 °C and used within 2 days.

Purification of Yeast Tubulin. (A) Initial Purification. Partial purification of yeast tubulin was achieved by the method of Barnes et al. (1992), with the following modifications described below. All steps were performed at 4 °C and included the protease inhibitor cocktails described by Barnes et al. (1992). Following cell disruption by bead-beating, the homogenate was first centrifuged for 10 min at 10000*g* in a GS3 rotor (Sorvall; RC5 centrifuge) to remove large particulates and cell debris. The supernatant from this centrifugation was then centrifuged at 100000*g* for 1 h (Beckman, 50.2 Ti rotor), as described by Barnes et al. (1992), to obtain a crude cell lysate. GTP was maintained at a concentration of 1 mM in the crude lysate, but was reduced to 0.1 mM in all subsequent steps and in all column buffers. The crude cell lysate was loaded onto a 50–70-mL DEAE-52 column (Whatman), washed with 5 column volumes of 0.1 M Pipes,[1] pH 6.9, 10 mM $MgCl_2$, and 2 mM EGTA (PME buffer) containing 10% glycerol and 0.16 M NaCl, and the tubulin eluted from the column with a single "step" of 0.6 M NaCl in PME buffer. The tubulin-containing fractions were precipitated by the addition of solid ammonium sulfate (375 mg mL^{-1}), pooled, and centrifuged (Sorvall SS34, 5000*g*, 10 min); the pellets were resuspended in 10 volumes of PME/0.1 mM GTP (plus protease inhibitors) and finally desalted over a Sephadex G25 column (2.5 cm × 30 cm). The desalted fractions were drop-frozen in liquid nitrogen and stored at

[1] Abbreviations: DIC microscopy, differential interference contrast microscopy; EGTA, ethylene glycol bis(β-aminoethyl ether)-*N,N,N′,N′*-tetraacetic acid; FPLC, fast protein liquid chromatography; MAPs, microtubule-associated-proteins; NDPK, nucleoside diphosphate kinase; Pipes, 1,4-piperazinediethanesulfonic acid.

–80 °C. This method routinely yielded a preparation which was 30% tubulin (Figure 1; Table II).

(*B*) *FPLC Purification.* Further purification of the tubulin from the DEAE-52 fractions was achieved using an anion-exchange FPLC column (Mono-Q; Pharmacia). The buffer which best resolved the tubulin from contaminants was PME, containing 50 μM GTP and a 0.16–1.0 M NaCl gradient. Prior to injection onto the column, the tubulin-containing sample was centrifuged at 14000*g* for 5 min in a microfuge. The FPLC apparatus, a 2-mL injection superloop, and the Mono-Q column itself were preequilibrated with PME, 50 μM GTP, and 0.16 M NaCl. We have used this method with both HR5*5 and HR10*10 columns (Pharmacia) and have found no significant differences.

To determine at what position the tubulin eluted from the column, we analyzed fractions by SDS–PAGE and silver staining (Switzer et al., 1979). The data reproducibly localized the tubulin-containing fractions to a single peak eluting at a salt concentration of 0.25–0.33 M NaCl. These fractions were immediately stabilized by adding 10% glycerol. The protein was then simultaneously desalted and concentrated in a Centricon 30 ultrafiltration cell by adding PME, 10% glycerol, and 50 μM GTP (no salt) and centrifuging (3000*g*, 3 h) until the tubulin concentration was 0.7–1.5 mg mL^{-1} prior to use. For long-term storage, we found the protein was more stable if it were first concentrated to 2 mg mL^{-1}, prior to being drop-frozen in liquid nitrogen and stored at –80 °C. For video-microscopy experiments, a slightly different procedure was used to concentrate the FPLC-purified tubulin. Solid ammonium sulfate (375 mg mL^{-1}) was added to the tubulin fractions and the precipitate pelleted (14000*g*, 10 min; microfuge) and desalted over a P10 column (Bio-Rad) equilibrated with PME/100 μM GTP (no glycerol). As the tubulin fractions eluted from the column, GTP was immediately added to 1 mM, and the samples were drop-frozen in liquid nitrogen prior to being stored at –80 °C.

Purification of Bovine Brain Tubulin. The MAP-free bovine brain tubulin used to obtain the dynamic parameters of individual microtubules *in vitro* was prepared as described previously (Mitchison & Kirschner, 1984). For the GTP hydrolysis data, the tubulin was initially isolated from three-cycle-purified MAP-rich microtubule protein by the method of Mitchison and Kirschner (1984). This was followed by FPLC chromatography as described for yeast, except that the Pipes concentration was reduced to 50 mM and NaCl was omitted from the buffer during protein loading onto the Mono-Q column.

Detection and Quantification of Microtubule Assembly. (*A*) *Immunofluorescence and Electron Microscopy Methods.* Microtubule assembly in aliquots of the FPLC-purified protein was carried out at 30 °C in PME, 10% glycerol, and 50 μM GTP and detected by one of two methods. Following assembly, the microtubules were fixed in 10–50 volumes of PME, 30% glycerol, and 1% glutaraldehyde and samples pipetted onto collodion-coated 50-mesh electron microscopy grids (Pelco Research Industries) and negatively stained with 1.5% uranyl acetate. The length distributions of the microtubules were determined as described previously (Farrell et al., 1987), using a Philips CM10 electron microscope.

Alternatively, aliquots of fixed microtubules were pipetted onto glass slides coated with poly(L-lysine) (0.1 mg/mL) and probed with monoclonal anti-α-tubulin antibodies (YL 1/2, YOL 1/34, Kilmartin et al., 1982; Mab077, Mab078, respectively; Accurate Chemical & Scientific Corp., Westbury, NY). After being stained with fluorescein- or rhodamine-conjugated goat secondary antibodies, the microtubules were visualized by fluorescence microscopy, using a Zeiss PM3 microscope at 1250× magnification.

(*B*) *Video-Enhanced Differential Interference Contrast Microscopy.* All experiments were carried out at 30 °C using FPLC-purified tubulin (0.5 mg mL^{-1}) in PME/1 mM GTP without glycerol. Microtubule assembly was initiated at the ends of *Strongylocentrotus purpuratus* axonemes, prepared according to the method of Bell et al. (1982), as modified by Walker et al. (1988). All measurements represent microtubule dynamic parameters at plus ends, defined as the axonemal ends at which microtubule growth was greater.

Video-enhanced microscopy was performed as described previously (Toso et al., 1993), using a Zeiss IM35 microscope at a final magnification of ca. 7500× and a temperature-controlled stage which allowed samples to be maintained at 30 °C ± 1 °C. The microtubule lengths were measured 30–70 min after assembly initiation, to ensure that the microtubules had achieved a steady state, and each microtubule length was measured 3 times using a "mouse" to trace an electronically overlaid cursor. Measurements from the video data were analyzed every 45 s using an IBM-compatible PC equipped with a Targa-M8 frame-grabber (Truevision) and JAVA video-analysis software (Jandel Scientific). A time interval of 45 s was chosen because the yeast microtubules grew far less quickly than vertebrate brain microtubules. For this reason, too, only those dynamic parameters which are independent of the window size can be used to compare yeast and vertebrate brain microtubules (e.g., see Table III). At least 14 microtubules from at least 3 experiments were used to obtained the data in Table III.

(*C*) *Terminology for Microtubule Dynamics.* Steady-state microtubule length data were analyzed using the following definitions. The limit of resolution of the microscope system was about 0.2 μm; therefore, any length change of less than 0.2 μm in 45 s (about 7.5 dimers s^{-1}) was scored as an **attenuation phase**. A **growth phase** was defined as an increase in microtubule length of greater than 0.2 μm in 45 s, whereas a **shortening phase** was classified as a decrease in length of greater than 0.2 μm in 45 s. Microtubule growing and shortening rates were calculated from the change in microtubule length divided by the 45-s interval. In some cases, however, microtubule disassembly was "catastrophic", and the microtubule disassembled completely within the 45-s window; in these instances, the disassembly rate was calculated from the microtubule length change divided by the time for the microtubule to disappear completely. **Dynamicity** is defined as the total number of dimers added and lost at a microtubule end in 1 s. The values in Table III represent average values calculated from the growing and shortening rates of all individual microtubules of the type observed. The microtubule **lifetime** is the total observation time of all microtubules of a given type (i.e., yeast or bovine brain); the proportion of the lifetime spent in the individual phases (growth, shortening, etc.) was then calculated from the ratios of the total times in the individual phases divided by the lifetime.

(*D*) *Turbidimetric Quantification of Microtubule Assembly in Small Volumes.* Because of the paucity of tubulin in yeast and the consequent low yield of tubulin from cell extracts (Table II), we examined whether microtubule assembly could be quantified in small sample volumes using a temperature-regulated plate reader (Ceres 900, Bio-Tek Instruments, Inc.). Microtubule assembly at 30 °C in 50–200-μL volumes of FPLC-purified tubulin (0.5–2.0 mg mL^{-1}) was followed at

340 nm using a 96-well half-area ($A/2$) plate. To evaluate whether the turbidimetric data accurately reflected the microtubule polymer mass, duplicate samples were also removed from the microplate wells 45 min after assembly initiation, the microtubules were sedimented (100000g, 30 min, SW50.1 rotor, Beckman), and the polymer mass in the pellets was measured by Bradford assay.

We found that above an optical density of about 0.003 the microtubule mass was linearly related to the turbidity (data not shown). In practical terms, we found that reproducible results were obtained with 100-μL volumes down to a tubulin concentration of approximately 0.5 mg mL^{-1}. Smaller volumes (50 μL) could be used; however, in this case, greater tubulin concentrations were necessary (about 0.8 mg mL^{-1}) to produce a turbidity which exceeded the sensitivity of the plate reader.

(*E*) *Determination of the Critical Concentration for Yeast Tubulin Assembly.* To measure the lowest concentration of free tubulin dimer required for microtubule formation, tubulin was polymerized in PME, 10% glycerol, and 50 μM GTP for 30 min at 30 °C over a tubulin concentration range of 0.025–1.5 mg mL^{-1}. Aliquots, 50 μL, were then centrifuged at 120000g for 30 min at 30 °C in an SW50.1 rotor (Beckman), and the protein in the supernatants and pellets (after resuspension in 50 μL of ice-cold buffer) was determined by Bradford assay (Bio-Rad). The amounts of protein in the pellets and supernatants were then plotted as a function of the initial protein concentration for assembly.

Determination of Yeast Tubulin Affinity for Mg–GTP. The most reproducible method for measuring the GTP-binding constant for yeast and bovine brain tubulins was that of Hummel and Dreyer (1962) as modified for tubulin by Levi et al. (1974). Briefly, 10–50-μL aliquots of a 1.1 mg mL^{-1} tubulin stock in PME/10% glycerol were gel-filtered at 4 °C at a flow rate of 0.7 mL min^{-1} over P-10 columns (22 cm × 1 cm) preequilibrated with PME, 10% glycerol, and [^{3}H]-GTP at a 7.5–1000 nM concentration range ([^{3}H]GTP specific activity varied between 55 and 7273 Ci M^{-1}). The stoichiometry of GTP binding to tubulin at each GTP concentration was determined by measuring the tubulin concentration (Bradford assay) and radiolabel (scintillation counting) eluting from the column in 0.5-mL fractions. The data were plotted in the form of a Scatchard plot (Scatchard, 1949), from which the equilibrium dissociation constant was determined by linear regression analysis of the data points.

Enzyme Assays. (*A*) *ATPase and GTPase Assays.* The activities of ATPases and GTPases in the fractions eluting from the FPLC column were determined by measuring P_i release from [γ-^{32}P]ATP and [γ-^{32}P]GTP, respectively, by the method of Penningroth et al. (1985). All reactions were performed at 30 °C in PME/10% glycerol plus 50–500 μM ATP or GTP ([ATP], 100 Ci M^{-1}; [GTP], 100 Ci M^{-1}). Briefly, 200-μL aliquots were taken from the FPLC column fractions and incubated with the appropriate radiolabeled nucleotide. At timed intervals, 10-μL samples were quenched in 400 μL of 6% (v/v) acetic acid, 2.5 mM KH_2PO_4, and 10% (w/v) activated charcoal ("quench solution"). The slurries were briefly mixed, and the charcoal-bound radiolabeled GTP was sedimented by centrifugation for 15 min in a microfuge. The γ-$^{32}P_i$ released into the supernatants by enzyme hydrolysis during the incubation period was then determined by scintillation counting.

To measure GTP hydrolysis during microtubule assembly, 100-μL aliquots of FPLC-purified tubulin (0.5–1.0 mg mL^{-1}) were incubated in PME, 10% glycerol, and 500 μM [γ-^{32}P]-GTP (10–20 Ci M^{-1}) at 30 °C. At timed intervals, 5-μL aliquots were quenched into 400 μL of quench solution, and the amount of P_i released was measured as described above. All GTP hydrolysis rates were corrected for the number of microtubule ends, which were obtained by determining the microtubule length distribution and polymer mass during assembly (Farrell et al., 1987).

(*B*) *Nucleoside Diphosphokinase Assay.* NDPK activity in the FPLC column fractions was measured by incubating 20-μL aliquots with 20 μL of PME/10% glycerol containing 1 mM [γ-^{32}P]ATP (100 Ci M^{-1}) and 0.1 mM GDP at 30 °C for 60 min. The reaction was quenched in 40 μL of 10% trichloroacetic acid, and the reaction products were separated by thin-layer chromatography using poly(ethylenimine)–cellulse plates (CEL 300 PEI; Brinkmann Instruments Inc.) developed with 1.0 M KH_2PO_4 and quantified by densitometric scanning of autoradiograms of the plates.

Table II: Purification of Yeast Tubulin[a]

purification step	total volume (mL)	total protein (mg)	total tubulin (mg)	tubulin content (%)	recovery (%)
crude cell lysate	1000	40000	24	0.06	100
DEAE-cellulose chromatography	60	32	10	30	42
ammonium sulfate precipitation	14	28	9	32	38
FPLC chromatography	9	9	9	>95	38

[a] The tubulin content of the protein fractions was determined by quantitative Western blot analysis using α-tubulin antibodies YL 1/2 and YOL 1/34 (Kilmartin et al., 1982).

RESULTS

Purification of Yeast Tubulin. The initial steps we used in the purification of yeast tubulin were essentially those described by Barnes et al. (1992) and involved fractionation of a yeast soluble protein extract by DEAE-cellulose ion-exchange chromatography. From approximately 88 L of cell culture, we obtained 40–80 g of crude cell lysate protein (Table II). A representative sample of the crude cell lysate, fractionated by SDS–PAGE, is shown in Figure 1a, lane 3; a distinct band corresponding to tubulin was not visible in this preparation by silver staining, and even in the corresponding immunoblot only a faint tubulin band was visible (Figure 1b, lane 3). This paucity of tubulin does not appear to result from tubulin sedimenting in the high-speed pellet (Figure 1a,b, lane 4). Following the DEAE chromatography step, however, which removed greater than 99% of the protein in the crude extract (Table II), immunoblot analyses with anti-α-tubulin antibodies showed that the tubulin was effectively bound by the column (Figure 1a,b, lane 5) and was significantly enriched in the fractions which eluted from the column with 0.6 M NaCl (to approximately 30% of the DEAE-bound protein; Table II, Figure 1a,b, lanes 6–9). When the tubulin was isolated from the *TUB2/tub2-590* heterozygote, an additional band was visible by SDS–PAGE, which migrated slightly faster than the major tubulin band (Figure 1a, lane 11). Immunoblot analysis with a rabbit polyclonal antibody raised against the C-terminal 12 amino acids of the *tub2-590* product confirmed that this band was truncated β-tubulin (data not shown). The slower-migrating tubulin band thus corresponded to the gene products of *TUB1*, *TUB2*, and *TUB3*, while the faster-migrating band corresponded to the *tub2-590* truncated β-tubulin.

Although tubulin was significantly enriched following DEAE-cellulose chromatography, this preparation was un-

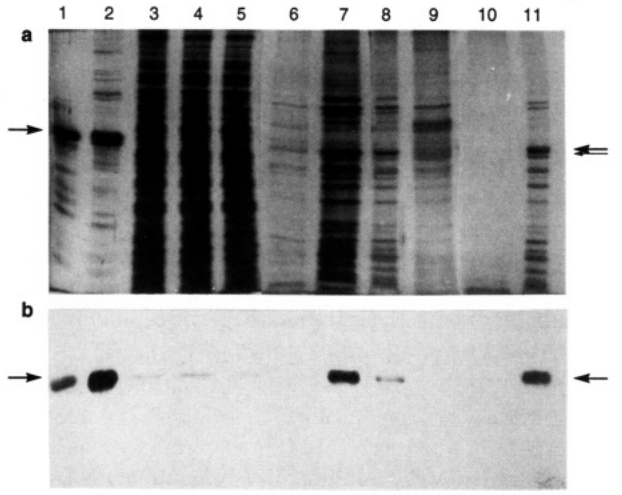

FIGURE 1: 10% SDS–PAGE analysis of protein fractions isolated from yeast cell lysates by the procedure of Barnes et al. (1992). (a) Silver-stained gel. (b) Corresponding Western blot of gel in (a) probed with anti-α-tubulin antibodies YL 1/2 and YOL 1/34. Lane 1, 0.25 μg of phosphocellulose-purified bovine brain tubulin; lane 2, 0.25 μg of FPLC-purified tubulin from ADY101-pADWT; lane 3, 5 μg of ADY101-pADWT cell lysate; lane 4, 5 μg of clarified cell lysate following high-speed centrifugation; lane 5, 5 μg of cell lysate fraction not bound to the DEAE-cellulose; lanes 6–9, four sequential tubulin-containing fractions eluted off the DEAE resin; these fractions were pooled and ammonium sulfate precipitated to give a supernatant (lane 10) and pellet (lane 11). The large arrow indicates the position of α-tubulin (from *TUB1* and *TUB3*) and wild-type β-tubulin (from *TUB2*). The smaller arrow indicates the position of the truncated form of β-tubulin (from *tub2-590*). The truncated tubulin is not visible in the immunoblot because an anti-α-tubulin antibody was used as probe.

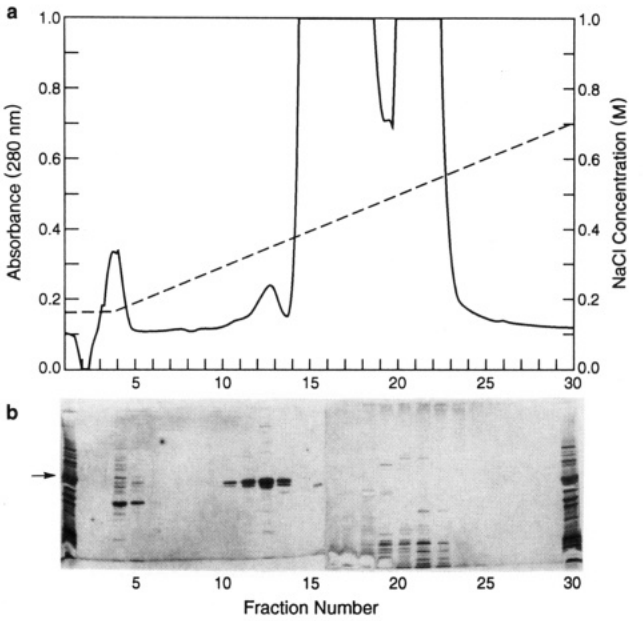

FIGURE 2: SDS–PAGE analysis of yeast tubulin purification by FPLC chromatography. (a) 0.5 mg of ADY101-pADWT cell lysate, purified by the method of Barnes et al. (1992), and containing about 30% tubulin (see lane 11, Figure 1), was fractionated on an HR5*5 Mono-Q column equilibrated in PME buffer containing 50 μM GTP, 10% glycerol, and 0.16 M NaCl. After being washed with 5 column volumes of buffer, the tubulin was eluted with a 0.16–0.7 M NaCl gradient, and 1-mL fractions were collected. (b) Silver-stained gel of 20-μL fractions in (a) resolved by 10% SDS–PAGE. Most of the contaminating RNA eluted in fractions 14–24, corresponding to the two large UV-absorbing peaks in (a). Tubulin eluted as the major component in fractions 10–13 (the tubulin position is shown by the arrow in panel b).

satisfactory for biochemical studies for several reasons. First, a major nonprotein contaminant was RNA (approximately 10 mg of RNA/mg of protein) which could not be removed by ammonium sulfate precipitation of the tubulin (data not shown). Tubulin polymerization in the DEAE-cellulose fractions was highly variable (data not shown; Barnes et al., 1992), presumably in part because of the inhibitory effects of polyanions on microtubule assembly (Bryan et al., 1975). This RNA also appeared to interfere with the ability of microtubules to adhere to the electron microscopy grids, since microtubule assembly in the DEAE-cellulose protein preparation was readily detectable by immunofluorescence microscopy (Materials and Methods), whereas no, or very few, microtubules were visible in duplicate samples prepared for electron microscopy. Treatment of the DEAE-cellulose fractions with a variety of RNases proved unsatisfactory, in part because of incomplete RNA digestion and also because the tubulin denatured during incubation at the temperatures required for efficient RNase activity. Initial experiments also revealed the presence of contaminating ATPase, GTPase, and NDPK activities in the DEAE-purified fractions, which would interfere with analyses of GTPase activities of tubulin mutations.

To obviate these problems, we fractionated the DEAE-cellulose-purified tubulin on a Mono-Q anion-exchange column by FPLC, using a 0.16–1.0 M NaCl linear gradient in PME buffer containing 50 μM GTP. The tubulin eluted as a single peak at 0.25–0.33 M NaCl and was clearly separated from the major UV-absorbing species (Figure 2a). SDS–PAGE analysis demonstrated that tubulin was the major component of the peak fractions, even after silver staining the gels (Figure 2b, fractions 10–13), and a quantitative analysis of gels stained with Coomassie blue revealed that the tubulin was 97% pure (data not shown). From 1.8 mg of DEAE-cellulose-purified protein (0.55 mg of tubulin) fractionated on the HR 5*5 FPLC column, we routinely obtained approximately 0.5 mg of tubulin. With a larger capacity column (HR 10*10), from about 15 mg of DEAE -cellulose-purified protein, approximately 5 mg of tubulin was routinely obtained. An important factor in obtaining a high yield of native tubulin was either the addition of 10% glycerol to the fractions immediately after they eluted from the column or, alternatively, precipitation of the tubulin with ammonium sulfate (0.375 g mL^{-1}).

Some variability among preparations of FPLC-purified tubulin was apparent with respect to a protein contaminant which migrated with a lower apparent molecular weight than tubulin (e.g., see Figure 5c, lanes 1 and 2). The level of this contaminant could be reduced by using a shallower NaCl gradient during FPLC (data not shown), or removed entirely by subjecting the tubulin to cycles of assembly–disassembly (Figure 5c, lanes 1–3). The tubulin was free of RNA, as determined by agarose gel electrophoresis of the tubulin-containing fractions and staining with ethidium bromide. Microtubule assembly in the FPLC-purified fractions also was reproducible, and the microtubules adhered to the electron microscopy grids, consistent with the idea that the RNA contaminating the Barnes et al. (1992) tubulin preparation was responsible for the inability of the microtubules to adhere to the electron microscopy grids.

The FPLC fractions from the experiment shown in Figure 2 were assayed for ATPase, GTPase, and NDPK activities (Figure 3). All three enzyme activities were prominent in the fractions which did not bind to the FPLC column (Figure 3, fractions 2–5), and some ATPase and GTPase activities were also evident in fractions corresponding to the major UV-absoring peaks (Figure 3, fractions 15–25). NDPK activity appeared to be restricted to the unbound fractions (Figure 3c,

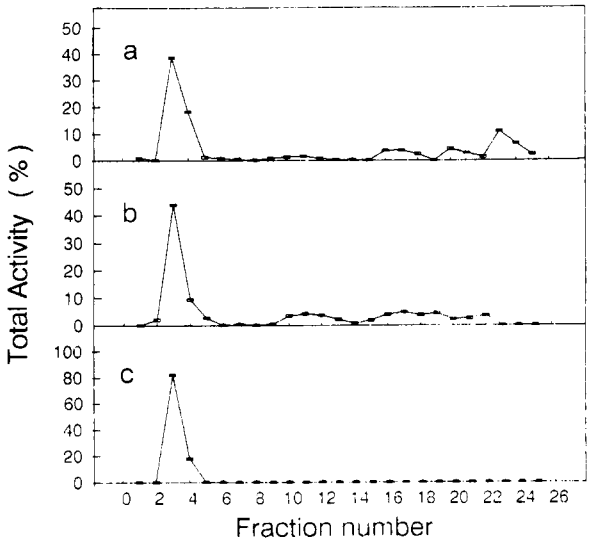

FIGURE 3: Analysis of the (a) ATPase, (b) GTPase, and (c) NDPK activities in the FPLC fractions of the experiment shown in Figure 2. The fractions not bound to the Mono-Q column (fractions 1–4) contained most of the enzymic activities. Tubulin eluted in fractions 10–13.

fractions 2–5). In contrast, only low GTPase activity was detected in the tubulin fractions (Figure 3b, fractions 10–13) at a level of approximately 0.25 min^{-1} at 30 °C under nonassembly conditions. This value is close to that which we obtained for phosphocellulose-purified bovine brain tubulin under identical conditions (0.15 min^{-1}, Table III), suggesting that the contaminating nucleoside triphosphatases had been effectively separated from the yeast tubulin.

Determination of the GTP-Binding Constant of Yeast Tubulin. FPLC-purified tubulin both from strain ADY103 (*TUB2/TUB2*) and from strain ADY101-pADWT (*TUB2/tub2-590*) was assayed using the equilibrium method of Hummel and Dreyer (1962), as modified for tubulin by Levi et al. (1974). The binding constants for tubulin isolated from the two yeast strains were essentially identical at approximately 1.6×10^7 M^{-1} (Figure 4a,b; Table III), demonstrating that the 12 amino acid truncation at the C-terminus of the *tub2-590* β-tubulin does not measurably influence GTP binding to the tubulin dimer. The yeast tubulin-binding constants were also slightly higher than that for phosphocellulose-purified bovine brain tubulin, measured under identical conditions (1.0×10^7 M^{-1}, Figure 4c; Table III). The stoichiometry of GTP binding to the two yeast tubulin preparations was approximately 1.0 mol of GTP per mole of tubulin dimer for both strains (Figure 4), indicating that significant denaturation of the tubulin did not occur during the purification procedure.

In Vitro Polymerization of Yeast Tubulin. Prior to initiation of polymerization, the FPLC-purified tubulin solution was concentrated using a Centricon-30 microconcentrator, and simultaneously the Mg^{2+} concentration was reduced from 10 to 1 mM by addition of 9 volumes of PME buffer without Mg^{2+}. The rationale for reducing the Mg^{2+} concentration derived from concern that the higher Mg^{2+} concentration would promote formation of nonmicrotubule tubulin polymers (Frigon & Timasheff, 1975); also because the contaminating RNA and other nucleoside triphosphatases had been removed by the FPLC step, competition with tubulin for Mg^{2+} binding was no longer a factor.

Incubation of the FPLC-purified tubulin solutions at 30 °C promoted the formation of *bona fide* microtubules, as determined by negative-stain electron microscopy (Figure 5a) and immunofluorescence light microscopy (Figure 5b). The protein could be taken through additional cycles of assembly–disassembly to yield microtubules composed essentially of pure tubulin, as determined by silver staining of SDS–PAGE gels (Figure 5c). A significant fraction (30%) of the tubulin, however, did not resolubilize after incubating the pelleted microtubules at 4 °C for 30 min (Figure 5c, lane 4). The reason for this is unclear, although electron microscopic examination of the cold-treated pellets revealed the presence of nonmicrotubule structures (Figure 5a, inset II) which may represent cold-stable tubulin aggregates.

Table III: Comparison of Yeast and Bovine Brain Tubulins[a]

parameter	tubulin source		
	ADY103 (*TUB2/TUB2*)	ADY101-pADWT (*TUB2/tub2-590*)	bovine brain (MAP-free)
K_a for GTP (M^{-1})	1.7×10^7	1.6×10^7	1.0×10^7
critical concn (mg mL^{-1})	0.10 ± 0.03	0.12 ± 0.04	0.56 ± 0.03
GTPase (min^{-1})			
nonassembly	0.25 ± 0.04	0.22 ± 0.03	0.15 ± 0.04
assembly	12800 ± 1800	14100 ± 700	21000 ± 2300
dynamic instability parameters at plus ends			
phase rates (s^{-1})			
growing	14.3 ± 1.4	16.3 ± 1.6	106 ± 13
shortening	12.1 ± 1.2	13.5 ± 2.8	104 ± 16
catastrophe	3004 ± 446	3272 ± 260	1464 ± 142
phase durations (s)			
growing	63.7 ± 4.5	56.2 ± 4.1	27.0 ● 3.0
shortening	45.0 ± 2.9	48.1 ± 3.1	20.0 ± 2.2
attenuation	74.7 ± 1.9	79.8 ± 5.8	21.3 ± 3.2
microtubule lifetime in			
growing phase	0.45 ± 0.02	0.38 ± 0.02	0.48 ± 0.05
shortening phase	0.04 ± 0.02	0.08 ± 0.03	0.35 ± 0.05
attenuation phase	0.51 ± 0.04	0.54 ± 0.02	0.19 ± 0.03
dynamicity (s^{-1})	19.4 ± 1.7	22.9 ± 2.2	83.0 ± 8.0
catastrophe frequency (s^{-1})	0.0012 ± 0.0001	0.0012 ± 0.0004	0.0005 ± 0.0002

[a] The heterozygous yeast strain CSY3-pCS3WT (*TUB2/tub2-590*), rather than ADY101-pADWT (also *TUB2/tub2-590*), was used as the tubulin source for determining the dynamic parameters of individual yeast microtubules reassembled from a heterozygous mutant. All dynamic parameters represent mean values obtained from 14–20 individual microtubules. The dynamic parameters for bovine brain microtubules are taken from Toso et al. (1993), except for the catastrophe rate. The values reported for the critical concentrations for assembly were obtained by linear regression analysis of the data points (*e.g.*, see Figure 5) and determination of ordinate intercepts. The values have not been corrected for the proportion of tubulin participating in assembly.

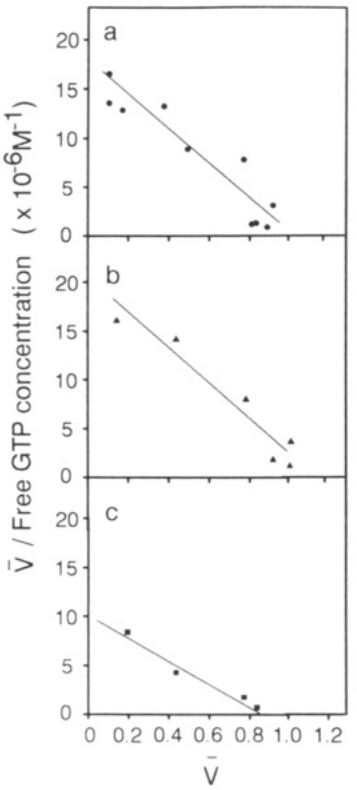

FIGURE 4: Determination of the equilibrium binding constants of yeast and bovine brain tubulins for Mg–GTP at 4 °C. Aliquots of FPLC-purified tubulin from (a) yeast ADY103 (*TUB2/TUB2*), (b) yeast ADY101-pADWT (*TUB2/tub2-590*), and (c) purified bovine brain tubulin were fractionated on 22 cm × 1 cm columns of Biogel P10 equilibrated with PME buffer containing 10% glycerol and between 7.5 and 1000 nM [^{3}H]GTP. Fractions, 0.5 mL, were collected, and the tubulin and radiolabeled nucleotide content was determined (Materials and Methods). The data are presented in the form of a Scatchard plot (1949) from which the binding constants were obtained. v is the molar stoichiometry of GTP bound to the tubulin dimer.

Critical Concentration for Yeast Tubulin Assembly. We measured the critical subunit concentration for tubulin polymerization using purified tubulin both from ADY103 (*TUB2/TUB2*) and from ADY101-pADWT (*TUB2/tub2-590*) by measuring the mass of microtubule polymer as a function of the initial tubulin concentration (Materials and Methods). For tubulin isolated from ADY103, a value of 0.10 mg mL^{-1} was obtained, while that for tubulin from ADY101-pADWT was 0.12 mg mL^{-1} (Figure 6a,b). Under identical experimental conditions, the critical concentration for phosphocellulose-purified bovine brain tubulin (0.56 mg mL^{-1}, data not shown) was significantly greater than either of the yeast tubulin preparations. A further notable difference between yeast and bovine brain tubulins was that the concentration of unpolymerized tubulin in the supernatant fraction was greater for yeast tubulin [cf. Figure 6 and Asnes and Wilson (1979)]. This may significantly increase the rescue frequency of yeast microtubules at higher tubulin concentrations (see Discussion).

GTPase Activity of Yeast Tubulin. The GTPase activity of yeast tubulin under both nonassembling and assembling conditions was measured to provide a reference for the effects of potential GTP-site mutations on the tubulin catalytic activity. For nonassembly conditions, FPLC-purified tubulin at concentrations of 29–70 μg mL^{-1}, below the critical concentration for assembly (Figure 6), was incubated with 50 μM [γ-^{32}P]GTP at 30 °C, and the rate of P_i release was measured (Materials and Methods). For tubulin isolated both

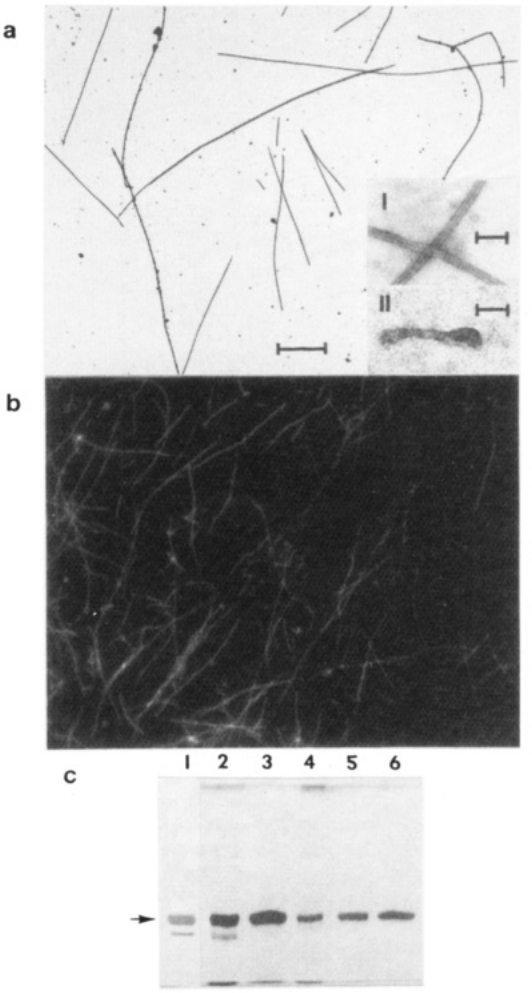

FIGURE 5: *In vitro* reassembly of yeast microtubules. FPLC-purified tubulin (0.5 mg mL^{-1}) isolated from strain ADY103 (*TUB2/TUB2*) was incubated for 45 min at 30 °C, and the reassembled microtubules were prepared for (a) electron microscopy by uranyl acetate negative staining (4140× magnification, bar = 2 μm; insets 24000× magnification, bar = 0.2 μm) or (b) immunofluorescence microscopy using anti-α-tubulin monoclonal antibody Mab077 as the primary antibody and a fluorescein-conjugated secondary antibody (1800× magnification). (c) FPLC-purified tubulin from ADY103 (0.8 mg mL^{-1}) was also subjected to cycles of assembly/disassembly, and samples were removed for SDS–PAGE analysis. The arrow identifies the band corresponding to tubulin in the silver-stained gel. Lane 1, 5 μg of the FPLC-purified tubulin; lane 2, 5 μg of the first warm supernatant; lane 3, 5 μg of the first warm pellet; the microtubule pellet was depolymerized at 4 °C and centrifuged to yield a pellet of cold-insoluble material (lane 4, 1 μg) and a supernatant of cold-soluble material. This material was subjected to a second assembly cycle to give a second warm supernatant (2 μg, lane 5) and pellet (2 μg, lane 6). Note the presence of a non-tubulin contaminant migrating ahead of the tubulin band (lanes 1 and 2), which could be removed by cycles of assembly/disassembly (lanes 3–6). A significant fraction of the microtubule pellets could not be resolubilized by incubation at 0 °C (lane 4) and contained many nonmicrotubule structures (inset II).

from ADY103 and from ADY101-pADWT, the rate of GTP hydrolysis was linear with time (for the 30-min observation period; data not shown) at 0.25 ± 0.04 and 0.22 ± 0.03 min^{-1}, respectively (Table III). These values were comparable to that of phosphocellulose-purified bovine brain tubulin which had also been purified by FPLC in a fashion identical to that of the yeast tubulins (0.15 ± 0.04 min^{-1} over a tubulin concentration range of 23–79 μg mL^{-1}, Table III).

To assay the tubulin GTPase activity under assembly conditions, 120-μL replicate samples of FPLC-purified tubulin at 0.5–1.5 mg mL^{-1}, from either ADY101-pADWT or

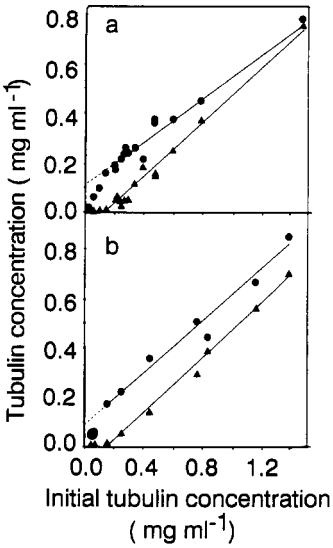

FIGURE 6: Determination of the critical concentrations for reassembly of yeast and bovine brain tubulins. Aliquots, 40 μL, of the different tubulins were incubated for 45 min at 30 °C over the indicated tubulin concentration ranges. The protein concentrations in the microtubule pellets (triangles) and supernatants (circles) were determined after sedimenting the microtubules at 100000*g* (Materials and Methods) and were plotted as a function of the initial tubulin concentration for assembly. The critical concentrations for assembly were determined from the ordinate intercepts of straight lines fitted to the data points by linear regression analysis. The values have not been corrected for the proportion of tubulin participating in assembly; this can be determined from the slopes of the regression lines fitted to the polymer mass data. (a) FPLC-purified tubulin from ADY103 (*TUB2/TUB2*); critical concentration = 0.10 mg mL^{-1}. (b) FPLC-purified tubulin from ADY101-pADWT (*TUB2/tub2-590*); critical concentration = 0.12 mg mL^{-1}.

ADY103, were incubated at 30 °C with 50 μM [γ-^{32}P]GTP in a 96-well microplate. At timed intervals, samples were removed to assay P_i release; samples were also taken for electron microscopy to determine the average microtubule length, from which the microtubule number concentration was calculated (Materials and Methods). Microtubule assembly was simultaneously measured turbidimetrically in one of the samples, from which the polymer mass was determined (Materials and Methods).

Following an initial lag period, during which time neither microtubule assembly nor P_i release was detected, P_i evolution proceeded at an initially rapid rate, corresponding to the rapid polymerization of microtubules to steady state (Figure 7a). At steady state, GTP hydrolysis proceeded linearly with time at a reduced rate, which thus appears to correspond to the steady-state turnover of subunits due to microtubule dynamic instability and treadmilling. When the initial rates of hydrolysis were corrected for the number of microtubule ends to obtain the assembly-dependent rates of GTP hydrolysis, average values of 12 800 ± 1800 min^{-1} (ADY103) and 14 100 ± 700 min^{-1} (ADY101-pADWT) were obtained. This represents a stimulation of greater than 10 000-fold over the nonassembly rate of tubulin GTP hydrolysis (Table III). Under identical conditions, bovine brain tubulin, purified first by phosphocellulose chromatography and subsequently by FPLC, gave an average value of 21 000 ± 2300 min^{-1} (Table III).

Interestingly, when the initial rate of P_i evolution per microtubule was compared with the initial rate of dimer addition per microtubule, calculated from the turbidity data, we found that an average of 9.1 ± 2.3 mol of P_i were released for every mole of tubulin dimer incorporated into the microtubule (Figure 7a). For comparison, we also measured

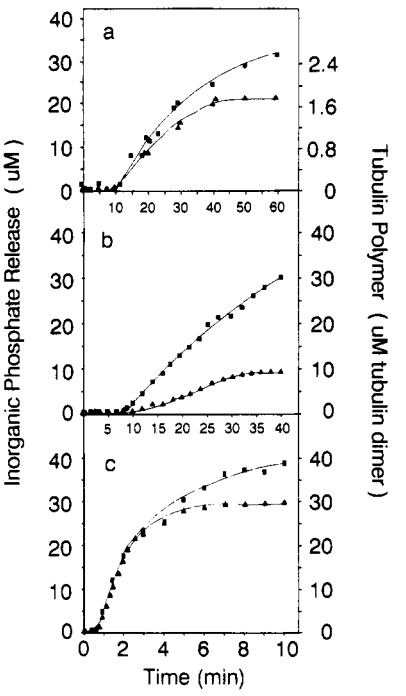

FIGURE 7: Tubulin–GTP hydrolysis during microtubule assembly. Microtubule formation was initiated in tubulin solutions in PME buffer containing 100 μM [γ-^{32}P]GTP and 10% glycerol by warming from 0 to 30 °C. Microtubule assembly was quantified turbidimetrically with a microplate reader (Materials and Methods). At timed intervals, 10-μL samples were removed to determine phosphate release (Materials and Methods). (a) 0.5 mg mL^{-1} tubulin isolated from wild-type ADY103 (*TUB2/TUB2*) by FPLC chromatography and one cycle of assembly/disassembly (e.g., see Figure 5c). (b) 2.2 mg mL^{-1} tubulin isolated from bovine brain by phosphocellulose chromatography, FPLC chromatography, and one cycle of assembly/disassembly. (c) 2.5 mg mL^{-1} MAP-rich bovine brain tubulin isolated by three cycles of assembly/disassembly. Note the superstoichiometric phosphate release during the initial, rapid phase of microtubule assembly in (a) (9.1 ± 2.3 mol of P_i/mol of assembled tubulin dimer) and (b) (3.7 ± 0.3 mol of P_i/mol of dimer). In contrast, in the MAP-rich preparation (c) phosphate release was essentially stoichiometric with dimer addition to the microtubules (1.08 ± 0.20). Triangles represent microtubule polymer mass determined turbidimetrically; squares represent inorganic phosphate release.

GTP hydrolysis during polymerization of phosphocellulose-purified bovine brain tubulin and also found P_i release to be superstoichiometric (3.7 ± 0.3 mol of P_i released per dimer incorporated, Figure 7b). In contrast, however, with MAP-rich bovine brain tubulin, P_i release during the initial stages of microtubule assembly was almost stoichiometric with subunit incorporation (1.08 ± 0.20, Figure 7c).

Dynamic Instability of Yeast Microtubules. Two methods were used to examine whether yeast microtubules exhibited dynamic instability *in vitro*. First, microtubules were assembled to steady state at three different initial tubulin concentrations (0.3, 0.5, and 1.5 mg mL^{-1}), and the length distributions of the microtubules were measured over a 120-min time course using electron microscopy.

The results are shown in Figure 8 for tubulin isolated from ADY103. Dynamic instability was apparent at all tubulin concentrations examined, as judged by microtubule length redistribution with time at steady state. Surprisingly, however, the extent of the length redistribution was dependent on the initial tubulin concentration. For example, at 0.3 mg mL^{-1} tubulin, the microtubule mean length was 1.5 μm 10 min after assembly initiation (the earliest time at which the microtubules reached steady state), and very few microtubules exceeded 5 μm in length. Two hours later, the microtubule

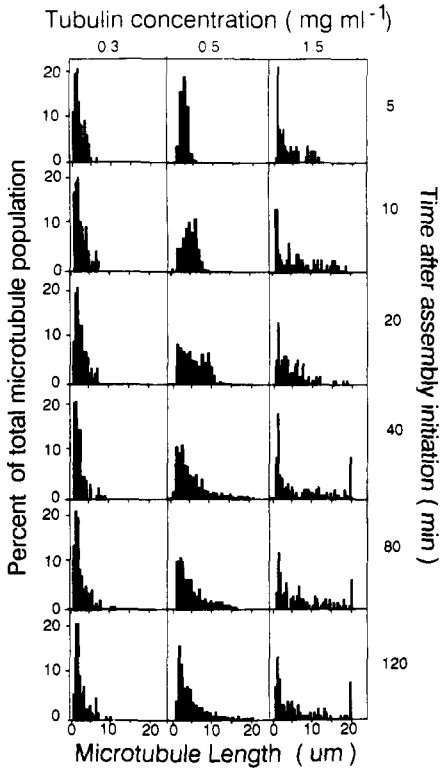

FIGURE 8: Length distributions of yeast microtubule populations *in vitro* as a function of time after assembly initiation. FPLC-purified tubulin from ADY103 was assembled at 30 °C in PME buffer containing 50 μM GTP and 10% glycerol at 0.3, 0.5, and 1.5 mg mL^{-1}. At the indicated times, 1-μL aliquots were removed for electron microscopy and the microtubule length distributions determined (Materials and Methods). At the lowest tubulin concentration, little redistribution of the microtubule lengths occurred after polymer mass steady state (at 10 min). In contrast, at the higher tubulin concentrations, a significant redistribution to longer microtubules occurred, indicative of dynamically unstable microtubules.

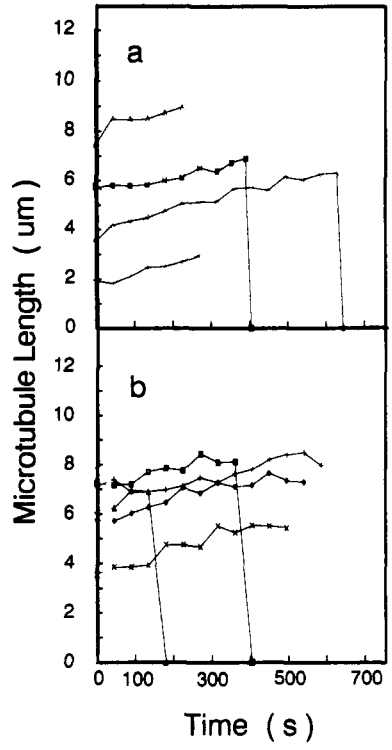

FIGURE 9: Dynamic instability of individual yeast microtubules *in vitro*. FPLC-purified tubulins from (a) ADY103 (*TUB2/TUB2*) and (b) CSY3-pCS3WT (*TUB2/tub2-590*), both at an initial concentration of 0.5 mg/mL, were assembled at 30 °C for 45 min in PME buffer containing 1 mM GTP. The length changes of individual microtubules were then quantified by DIC video microscopy (Materials and Methods). Four representative microtubules from each tubulin preparation are shown.

mean length was still only 2 μm, only 15% of the microtubules exceeded a length of 5 μm, and no microtubules longer than 10 μm were observed. In contrast, at an initial tubulin concentration of 1.5 mg mL^{-1}, the microtubule average length was 5.9 μm 10 min after assembly initiation, but increased to 7.3 μm at 120 min and 14% of the microtubules exceeded 10 μm.

Microtubule dynamic instability at plus ends was also readily visualized when the length changes of individual microtubules were monitored in real time using video-enhanced DIC microscopy. Representative examples are given of individual microtubules reassembled from wild-type tubulin (ADY103, *TUB2/TUB2*, Figure 9a) and from tubulin composed of an equal mixture of wild-type dimers and dimers carrying the truncated β-subunit (CSY3-pCS3wt, *TUB2/tub2-590*, Figure 9b). For both tubulin samples, individual microtubules behaved qualitatively like MAP-free vertebrate brain microtubules and exhibited random growing and shortening length changes characteristic of dynamically unstable microtubules (Mitchison & Kirschner, 1984; Horio & Hotani, 1986; Walker et al., 1988). The two yeast tubulins behaved substantially the same, with the major difference being that microtubules containing dimers with the truncated β-subunit spent a slightly greater proportion of their "lifetimes" in the shortening phase (0.08 versus 0.04) and slightly less in the growing phase (0.38 versus 0.45) (Table III).

Interestingly, a "rescue" event, in which a catastrophically disassembling microtubule transitioned to a growing or attenuation phase, was rarely observed with either preparation of yeast microtubules. This contrasts with the behavior of MAP-free bovine brain microtubules, where rescues frequently occur [e.g., see Walker et al. (1988) and Toso et al. (1993)]. In addition, for yeast microtubules, the frequency with which catastrophic depolymerization occurred was somewhat greater than that for bovine brain microtubules under the same conditions (0.0012 versus 0.0005 s^{-1}, Table III). Generally, however, the yeast microtubules were far less dynamic than MAP-free brain microtubules, with approximately 4-fold fewer total events occurring at a microtubule end in a given period ("dynamicity", Table III).

DISCUSSION

Purification of Yeast Tubulin. Our goal has been to develop yeast as an experimental genetic system in which the biochemistry of yeast tubulin could be studied with acceptable facility. The ability to characterize yeast tubulin biochemically would then complement the exceptional molecular biology of this organism and make it possible to pursue, by a combination of mutagenesis and biochemical methods, a functional analysis of tubulin sites. Our particular motivation for the present study stemmed from an interest in defining the β-tubulin sites involved with the binding and hydrolysis of GTP; consequently, we have emphasized these properties of tubulin in this study. In principle, however, the tubulin purification scheme described in the present work will be applicable to the biochemical study of any selected tubulin site, such as a drug-binding site.

The first method for purifying milligram quantities of tubulin from yeast was recently described by Barnes et al. (1992). Although the tubulin was assembly-competent and formed *bona fide* microtubules *in vitro*, the efficiency of microtubule formation was quite variable among preparations,

most likely because of the large amounts of contaminating RNA (Figure 2a, Bryan et al., 1975). In initial experiments, we found that tubulin prepared by the method of Barnes et al. (1992) was also contaminated with significant levels of other GTPases, ATPases, and kinases (data not shown); such contaminating activities would have precluded using the preparations to analyze the effects of potential GTP-site mutations on yeast tubulin GTPase activity.

We found, however, that when yeast tubulin, isolated by the Barnes et al. (1992) method, was further purified by FPLC, it exhibited minimal non-assembly-related GTPase activity (0.22–0.25 min^{-1}; Figure 3b, Table III). This activity was comparable to that measured for phosphocellulose-purified bovine brain tubulin after fractionation by FPLC (0.15 min^{-1}, Table III). Similarly, no significant ATPase or nucleoside diphosphokinase activities were detected in the FPLC-purified yeast tubulin preparations (Figure 3a,c).

In addition, the nucleic acid contaminants (predominantly RNA) were also removed by the FPLC step, since ethidium bromide staining of a tubulin sample fractionated by agarose gel electrophoresis showed no evidence of nucleic acid (data not shown). The FPLC-purified tubulin reliably and efficiently assembled *in vitro* (Figure 5), supporting the idea that the nucleic acid contamination contributed to the variable microtubule assembly in the Barnes et al. (1992) preparations (Bryan et al., 1975). No significant differences in the behavior of tubulins, isolated either from the ADY103 (*TUB2/TUB2*) strain of yeast or from the transformed ADY101-pADWT (*TUB2/tub2-590*) strain, were detected during the Barnes et al. (1992) or FPLC purification steps.

From approximately 88 L of yeast culture (1–2 kg wet weight of cells), the FPLC procedure routinely yielded 5–10 mg of >95% purified tubulin. By comparison, from a 300-g bovine brain, we normally obtain approximately 80 mg of microtubule protein, consisting of 70% tubulin and 30% MAPs. The low quantities of yeast tubulin obtained by this method do not present an insurmountable problem for assembly studies, because the polymerization of only 40–50 μg of tubulin can be quantified turbidimetrically with a Ceres 900 microplate reader.

GTP-Binding Properties of Yeast Tubulin. Yeast tubulin both from ADY103- and from ADY101-transformed strains bound GTP with a stoichiometry approaching 1 mol of GTP/mol of tubulin dimer (Figure 4), demonstrating that the tubulin does not significantly denature during the purification step. Furthermore, tubulin isolated from the two strains bound GTP with a similar, high affinity (1.6×10^7 M^{-1}; Figure 4a,b, Table III), comparable with that of phosphocellulose-purified bovine brain tubulin (1.0×10^7 M^{-1}; Figure 4c, Table III). The similarity of the GTP-binding constants for tubulins isolated from the 2 yeast strains also indicates that the 12 C-terminal amino acids deleted from the *tub2-590* β-tubulin do not play a significant role in GTP binding to the tubulin dimer.

It has been shown previously that truncation of the C-terminal 27 amino acids of yeast β-tubulin does not prevent microtubule formation at normal growth temperatures (Matsuzaki et al., 1988). Although the GTP-binding affinity of the truncated tubulin was not compared with that of wild-type tubulin, the assembly competence of the truncated tubulin is consistent with the idea that the C-terminal region of β-tubulin is not directly involved with GTP binding to the tubulin dimer. It is notable, too, that attempts to locate the β-tubulin sequences involved with GTP binding, using both GTP cross-linking and primary sequence comparisons, have not identified the C-terminal region of β-tubulin as being involved with the GTP-binding site [reviewed in Burns et al. (1993)].

In Vitro Assembly of Yeast Tubulin. (A) General Properties. In contrast to the essentially identical GTP-binding properties of dimers composed of the wild-type and truncated yeast β-tubulins, there are differences in the assembly properties of the two tubulins. Wild-type tubulin isolated from strain ADY103 (*TUB2/TUB2*) assembled with a critical concentration in glycerol-containing buffer of 0.10 mg mL^{-1} (Figure 6a). However, tubulin from the transformed ADY101 heterozygote (*TUB2/tub2-590*), composed of a mixture of wild-type dimers and dimers carrying the *tub2-590* truncated β-tubulin, had a slightly greater critical concentration under identical conditions (0.12 mg mL^{-1}, Figure 6b). This small increase, if significant, must derive from the presence of dimers composed of the *tub2-590* truncated β-tubulin and may underestimate the critical concentration of a "pure" solution of dimers carrying only the truncated β-tubulin subunit (*i.e.*, from a *tub2-590/tub2-590* homozygote). Other work has shown that cells carrying *tub2-590* exhibit increased sensitivity to microtubule-depolymerizing drugs (Katz & Solomon, 1988) as do yeast cells in which the C-terminal 27 amino acids of β-tubulin have been deleted (Matsuzaki et al., 1988). In mammalian cells, too, mutations in the C-terminus of β-tubulin affect microtubule formation (Boggs et al., 1988). Together these data indicate that the C-terminal region of β-tubulin, while not affecting GTP binding to the tubulin dimer, plays an important role in the affinity of the dimer for the microtubule end.

Tubulin from both ADY103 and transformed ADY101 strains could be purified by subjecting the protein to warm assembly/cold disassembly cycles to yield tubulin which was essentially pure by silver staining of SDS–PAGE gels (Figure 5c). We found, however, that approximately 30% of the tubulin did not resolubilize after incubation for 60 min at 0 °C (Figure 5c, lane 4). Incubation of the microtubule pellets for longer times (as long as 180 min) at 0 °C did increase the fraction of tubulin solubilized (to approximately 85%); however, a substantial fraction of the tubulin still failed to solubilize. The reason for this is not known, although cold-stable microtubules have been reported previously during cycling of vertebrate brain tubulin and were attributed to the presence of a MAP which conferred cold-stability to the microtubules (Margolis et al., 1990). Certainly, the cold-stable yeast microtubule pellets contain other proteins (Figure 5c, lane 4) which could act equivalently to the mammalian protein, but we have not yet investigated this further.

(B) Dynamic Instability of Yeast Microtubules. The results of experiments in which the time-dependent length changes were followed both of microtubule populations (Figure 8) and at the plus ends of individual microtubules (Figure 9) clearly demonstrate that yeast microtubules exhibit the steady-state random changes in length indicative of dynamic instability. Microtubules reassembled from ADY103 (*TUB2/TUB2*) and from CSY3-pCS3WT (*TUB2/tub2-590*) showed little difference with respect to the growing and shortening rates, including catastrophic disassembly rates, as well as with respect to the average durations of the growing and shortening phases (Table III). Similarly, the average duration of the "attenuation" phase, during which time no change in the microtubule length was detectable, was similar for microtubules from both sources.

The only detectable difference between the two microtubule preparations was that microtubules reassembled from CSY3-

pCS3WT tubulin tended to spend a slightly smaller proportion of their "lifetimes" in the growth phase (0.38 versus 0.45) and proportionately more time in the shortening phase (0.08 versus 0.04) (Table III). Although these differences are consistent with the slightly greater critical concentration for assembly of tubulin isolated from *tub2-590* strains, when compared with *TUB2* wild-type strains (Figure 6), as well as with their greater drug sensitivity (Katz & Solomon, 1988), the data should be interpreted with caution owing to the relatively large error limits.

In contrast, the dynamics of individual microtubules from both yeast strains were markedly different from those of bovine brain microtubules under the same conditions. Overall, the yeast microtubules were far less dynamic than brain microtubules, with approximately 4-fold fewer total events occurring at the microtubule plus ends per unit time ("dynamicity": 19.4 versus 83.0 s^{-1}, Table III). This difference in dynamicities between the yeast and brain microtubules was caused in large part because both the growing and noncatastrophic shortening rates of yeast microtubules were much smaller than those of brain microtubules (Table III). The smaller growing and shortening rates were reflected in the shorter length changes ("excursions") of the yeast microtubules, which generally amounted to only about a micrometer of length (Figure 9); with brain microtubules, by comparison, excursions of tens of micrometers are possible (data not shown; Toso et al., 1993).

When compared with brain microtubules, yeast microtubules also spent a far greater proportion of their lifetime in the attenuation phase (0.51–0.54 versus 0.19), in which length changes were not observed, and a far smaller proportion of their lifetimes in the shortening phase (0.04–0.08 vs 0.35) (Table III). Consequently, yeast microtubules tended to become longer with time at steady state until a catastrophic shortening event caused their complete disassembly (Figure 9).

A further striking difference between yeast and brain microtubules was that yeast microtubules were rarely rescued from catastrophic shortening and usually depolymerized completely, back to the axonemal seed (Figure 9); with brain microtubules, in contrast, rescues of rapidly disassembling microtubules occurred frequently (data not shown; Toso et al., 1993). The rarity of rescues with yeast microtubules may explain why there was relatively little increase in the average length of microtubules at steady state when assembled at low tubulin concentrations (Figure 8, 0.3 mg mL^{-1} tubulin). At the higher initial tubulin concentration for assembly (1.5 mg mL^{-1}), in contrast, there was a significant increase in the average length of microtubules at steady state (Figure 8). This may be related to the higher concentration of unassembled tubulin at 1.5 mg mL^{-1} (Figure 6), possibly by increasing the rescue frequency.

Modulation of microtubule rescue may be a general mechanism for regulating microtubule dynamics and function. A reduction in microtubule rescue frequency was seen in interphase extracts of *Xenopus* oocytes by the addition of okadaic acid, an inhibitor of phosphatase activity (Gliksman et al., 1992). As a consequence, the microtubule length distribution was biased toward shorter microtubules, in much the same way as that of yeast microtubules (Figure 8). In yeast cells, the short, transitory mitotic spindle and the lack of an extensive, persistent, interphase network of microtubules may thus be accomplished in part by the infrequent rescues of the microtubules.

GTPase Activity of Yeast Tubulin. As reported previously for vertebrate brain tubulin [*e.g.*, see Andreu and Timasheff (1981)], assembly of yeast tubulin into microtubules was accompanied by a stimulation of the tubulin GTPase activity. Following an initial lag period, during which time neither microtubule assembly nor phosphate evolution was detected, there was an initially rapid polymerization of microtubules and a coincident increase in phosphate evolution (Figure 7a). The phosphate evolution rate, when corrected for the number of microtubule ends, represented a stimulation in the tubulin GTPase activity of several orders of magnitude when compared with the GTPase activity of unassembled tubulin dimers (Table III). After the attainment of polymer mass steady state, phosphate evolution continued at a slower, linear rate which presumably reflected the steady-state turnover of tubulin subunits by treadmilling and dynamic instability.

The superstoichiometric phosphate release during the initial, rapid phase of microtubule formation (Figure 7) suggests that tubulin subunit addition to microtubule ends, even during rapid assembly, is highly inefficient in the absence of MAPs. In the case of yeast microtubules, for example, the data indicate that for every tubulin subunit incorporated into a microtubule approximately eight GTP dimers add to the microtubule, hydrolyze the GTP, and dissociate nonproductively from the microtubule end. Similarly, for bovine brain phosphocellulose-purified microtubules, about four GTP dimers must add to the microtubule end to achieve the incorporation of one subunit.

The superstoichiometric phosphate release does not appear to derive from GTP hydrolysis by nonmicrotubule structures, such as protofilament sheets. Examination of the yeast preparations by electron microscopy during assembly revealed that microtubules were the predominant structures (*e.g.*, see Figure 5a); certainly there were insufficient nonmicrotubule structures to account for all of the superstoichiometric phosphate release. This would amount to nearly 90% of the total phosphate release, assuming that microtubule assembly hydrolyzed only one phosphate per dimer incorporated into the microtubule. Formally, however, we cannot exclude the possibility that some of the phosphate release derived from structures other than microtubules; the superstoichiometric values must therefore be regarded as maximum estimates of the microtubule-related GTP hydrolysis.

The simplest explanation for the inefficiency of subunit addition is that significant microtubule growing and shortening (dynamic instability) still occur even under conditions of rapid microtubule growth. Repeated cycles of tubulin–GTP addition to microtubules, followed by GTP hydrolysis and subsequent loss of tubulin–GDP subunits, would account for the superstoichiometric phosphate release. Using DIC video microscopy, we found no evidence for dynamic instability during microtubule growth, but the stoichiometry of phosphate release (Figure 7) indicates that the extent of microtubule growing and shortening amounts to only a few subunits under these conditions and excursions of such small size would not be detectable by this method (data not shown).

Frequent periods in which microtubules grow and shorten by only a few subunits ("micro-excursions") also account for the apparent inconsistency that yeast microtubules hydrolyze at least as much GTP as bovine brain microtubules during polymerization (Figure 7a,b), but appear less dynamic than their brain counterparts when observed by DIC video microscopy (Table III). Yeast microtubules may thus be as dynamic as the brain microtubules, in terms of excursion frequency, but for yeast microtubules, a far greater proportion of the length changes would not be seen and would be scored

as an "attenuation". This would give rise to the perception that yeast microtubules are less dynamic, have longer attenuation phases, and spend a greater proportion of their "lifetimes" in the attenuation phase than do brain microtubules (Table III).

In the presence of MAPs, by contrast, dynamic instability is suppressed (Horio & Hotani, 1986; Farrell et al., 1987) and phosphate release is almost stoichiometric with subunit addition (Figure 7c), indicating that MAPs promote the efficiency of microtubule assembly by reducing the probability of subunit loss from the microtubule following GTP hydrolysis. This would be consistent with the observation that the dimer dissociation rate constant is smaller for MAP-rich microtubules than for MAP-free microtubules (Farrell et al., 1983).

The superstoichiometric release of phosphate during the initial stages of assembly of yeast and MAP-free brain microtubules is difficult to reconcile with the substoichiometric phosphate release observed by other workers, which has been interpreted in terms of a large stabilizing "cap" of tubulin–GTP subunits at the microtubule end, numbering in the hundreds or even thousands [*e.g.*, see Carlier and Pantaloni (1981) and Carlier et al. (1987)]. There is still considerable controversy as to both the existence and the size of the proposed "cap" [*e.g.*, see Burns (1991), Carlier et al. (1987), O'Brien et al. (1987), and Stewart et al. (1990)] and the data presented in this paper appear incompatible with a substantial tubulin–GTP cap.

One methodological difference between our experiments and those of Carlier and co-workers is that we use 1 M glycerol in our assembly buffers, in contrast to the 3.4 M glycerol generally used by the Carlier group. Possibly, the greater glycerol concentration used by the Carlier group suppresses dynamic instability excursions, thereby making tubulin–GTP subunit addition to microtubules more efficient and the detection of a tubulin–GTP cap easier. With MAP-rich microtubules, in which dynamic instability is to a large extent suppressed (Farrell et al., 1987), the reduction of phosphate release to near-stoichiometric with tubulin addition is generally consistent with the idea that factors which suppress dynamic instability may also reduce the stoichiometry of phosphate release during microtubule assembly.

In conclusion, yeast tubulin isolated as described in this report exhibits all of the qualitative characteristics of vertebrate brain tubulins; however, there are significant quantitative differences between the yeast and brain tubulins, primarily with respect to their assembly properties. The differences seem to derive from differences in the tubulins themselves, rather than from the actions of associated proteins, since both tubulins were highly purified. This conclusion is not too surprising considering the substantially different primary sequences and drug-binding properties of the two tubulins. The data also demonstrate the feasibility of using yeast as a system for studying the biochemistry of tubulin. In conjunction with the outstanding molecular genetics of yeast, it should now be possible to pursue a structure–function analysis of tubulin domains in this organism.

ACKNOWLEDGMENT

We thank Dr. Georjana Barnes for making available prior to publication the protocol for isolating yeast tubulin. We also thank Dr. Monty Raedeke for advice with the FPLC and Ms. Cindy Dougherty and Drs. Mary Anne Jordan and Kim Middleton for helpful discussion. We also thank Mr. Herb Miller for providing the bovine brain tubulin used in this work.

REFERENCES

Andreu, J. M., & Timasheff, S. N. (1981) *Arch. Biochem. Biophys. 211*, 151–157.
Asnes, C. F., & Wilson, L. (1979) *Anal. Biochem. 98*, 64–73.
Barnes, G., Louie, K. A., & Botstein, D. (1992) *Mol. Biol. Cell 1*, 1–19.
Bell, C. W., Fraser, C., Sale, W. S., Tang, W. Y., & Gibbons, I. R. (1982) *Methods Cell Biol. 24*, 373–397.
Boggs, B. A., Minotti, A. M., Loeb, L. M., Cook, R., & Cabral, F. (1988) *J. Biol. Chem. 263*, 14566–14573.
Bryan, J., & Wilson, L. (1971) *Proc. Natl. Acad. Sci. U.S.A. 68*, 1762–1766.
Bryan, J., Nagle, B. W., & Doenges, K. H. (1975) *Proc. Natl. Acad. Sci. U.S.A. 72*, 3570–3574.
Burke, D., Gasdaska, P., & Hartwell, L. (1989) *Mol. Cell. Biol. 9*, 1049–1059.
Burns, R. G. (1991) *Biochem. J. 277*, 239–243.
Burns, R. G. (1992) *FEBS Lett. 297*, 205–208.
Burns, R. G., Farrell, K. W., & Surridge, C. D. (1993) in *G-Proteins* (McCormick, F., Ed.) Ciba Foundation Proc., London (in press).
Cabral, F. (1983) *J. Cell Biol. 97*, 22–29.
Carlier, M.-F., & Pantaloni, D. (1981) *Biochemistry 20*, 1918–1924.
Carlier, M.-F., Didry, D., & Pantaloni, D. (1987) *Biochemistry 26*, 4428–4437.
Chang, S. C., & Flavin, M. (1988) *Cell Motil. Cytoskel. 10*, 400–409.
Correia, J. J. (1991) *Pharmacol. Ther. 52*, 127–147.
Dustin, P. (1984) in *Microtubules*, 2nd ed., Springer-Verlag, Berlin, Heidelberg, and New York.
Farrell, K. W., Himes, R. H., Jordan, M. A., & Wilson, L. (1983) *J. Biol. Chem. 258*, 14148–14156.
Farrell, K. W., Jordan, M. A., Miller, H. P., & Wilson, L. (1987) *J. Cell Biol. 104*, 1035–1046.
Frigon, R. P., & Timasheff, S. N. (1975) *Biochemistry 14*, 4559–4566.
Gliksman, N. R., Parsons, S. F., & Salmon, E. D. (1992) *J. Cell Biol. 119*, 1271–1276.
Hayden, J. H., Bowser, S. S., & Rieder, C. L. (1990) *J. Cell Biol. 111*, 1039–1045.
Horio, T., & Hotani, H. (1986) *Nature 321*, 605–607.
Huffaker, T. C., Hoyt, M. A., & Botstein, D. (1987) *Annu. Rev. Genet. 21*, 259–284.
Hummel, J. P., & Dreyer, W. J. (1962) *Biochim. Biophys. Acta 63*, 530–532.
Kaslow, H. R., Groppi, V. E., Abood, M. E., & Bourne, H. R. (1981) *J. Cell Biol. 91*, 410–413.
Katz, W., & Solomon, F. (1988) *Mol. Cell. Biol. 8*, 2730–2736.
Katz, W., Weinstein, B., & Solomon, F. (1990) *Mol. Cell. Biol. 10*, 5286–5294.
Kilmartin, J. V., Wright, B., & Milstein, C. (1982) *J. Cell Biol. 93*, 576–582.
Kirschner, M., & Mitchison, T. J. (1986) *Cell 45*, 329–342.
Levi, A., Cimino, M., Mercanti, D., & Calissano, P. (1974) *Biochim. Biophys. Acta 365*, 450–453.
L'Hernault, S. W., & Rosenbaum, J. L. (1985) *Biochemistry 24*, 473–478.
Lim, L.-K., Sekura, R., & Kaslow, H. R. (1985) *J. Biol. Chem. 260*, 2585–2588.
Margolis, R. L., & Wilson, L. (1978) *Cell 13*, 1–8.
Margolis, R. L., Rauch, C. T., Pirollet, C. T., & Job, D. (1990) *EMBO J. 9*, 4095–4102.
Matsuzaki, F., Matsumoto, S., & Yahara, I. (1988) *J. Cell Biol. 107*, 1427–1435.
Mejillano, M. R., Barton, J. S., & Himes, R. H. (1990) *Biochem. Biophys. Res. Commun. 166*, 653–660.
Mitchison, T. J. (1988) *Annu. Rev. Cell Biol. 4*, 527–549.
Mitchison, T. J. (1989) *J. Cell Biol. 109*, 637–652.

Mitchison, T. J., & Kirschner, M. (1984) *Nature (London) 312*, 237–242.
Mitchison, T. J., Evans, L., Schulze, E., & Kirschner, M. (1986) *Cell 45*, 512–547.
Neff, N. F., Thomas, J. H., Grisafi, P., & Botstein, D. (1983) *Cell 33*, 211–219.
Oakley, B. R., & Morris, N. R. (1980) *Cell 19*, 255–262.
Oakley, C. E., & Oakley, B. R. (1989) *Nature 338*, 662–664.
Oakley, B. R., Oakley, C. E., Yoon, Y., & Yung, M. K. (1990) *Cell 61*, 1289–1301.
O'Brien, E. T., Voter, W. A., & Erickson, H. P. (1987) *Biochemistry 26*, 4148–4156.
Penningroth, S. M., Rose, P., Cheung, A., Peterson, D. D., Rothacker, D. Q., & Bershak, P. (1985) *Cell Motil. 5*, 61–75.
Raybin, D., & Flavin, M. (1977) *J. Cell Biol. 73*, 492–504.
Rieder, C. L., & Alexander, S. P. (1990) *J. Cell Biol. 110*, 81–95.
Scaife, R. M., Wilson, L., & Purich, D. L. (1992) *Biochemistry 31*, 310–316.
Scatchard, G. (1949) *Ann. N.Y. Acad. Sci. 51*, 660–672.
Schatz, P. J., Pillus, L., Grisafi, P., Solomon, F., & Botstein, D. (1986) *Mol. Cell. Biol. 6*, 3711–3721.
Sherman, F., Fink, G. R., & Hicks, J. B. (1986) in *Laboratory Course Manual for Methods in Yeast Genetics*, Cold Spring Harbor Laboratory, Cold Spring Harbor, NY.
Sternlicht, H., Yaffe, M. B., & Farr, G. W. (1987) *FEBS Lett. 214*, 226–235.
Stewart, R. J., & Farrell, K. W., & Wilson, L. (1990) *Biochemistry 29*, 6489–6498.
Switzer, R. C., Merril, C. R., & Shifrin, S. (1979) *Anal. Biochem. 96*, 231–237.
Toso, R. J., Jordan, M. A., Farrell, K. W., Matsumoto, B., & Wilson, L. (1993) *Biochemistry 32*, 1285–1293.
Walker, R. A., O'Brien, E. T., Pryer, N. K., Soboeiro, M. F., Boter, W. A., Erickson, H. P., & Salmon, E. D. (1988) *J. Cell Biol. 107*, 1437–1448.
Wegner, A. (1976) *J. Mol. Biol. 108*, 139–150.
Weisenberg, R. C. (1972) *Science 177*, 1104–1105.
Weisenberg, R. C., Borisy, G. G., & Taylor, E. W. (1968) *Biochemistry 7*, 4466–4478.
Weisenberg, R. C., Deery, W. J., & Dickinson, P. J. (1976) *Biochemistry 15*, 4248–4254.